Int J Adv Manuf Technol (2006) 28: 321–327
DOI 10.1007/s00170-004-2363-5

ORIGINAL ARTICLE

Wenming Zhang · Guang Meng · Hongguang Li

Adaptive vibration control of micro-cantilever beam with piezoelectric actuator in MEMS

Received: 17 July 2004 / Accepted: 31 July 2004 / Published online: 1 June 2005

Abstract This paper proposes a dynamical model and the governing equations of motion of the micro-cantilever beams based MEMS with piezoelectric actuator (PZT). The Rayleigh–Ritz method is used to reduce the order of the system and the state equations are presented in modal space. The first ten mode frequencies and mode shapes of the micro-cantilever beam with and without PZT are studied. The effects of PZT on the modal frequencies and shapes of the beam system can be ignored for the reason that the beam holds larger nature frequencies and Q values in micro-scale. A rational linearizing feedback controller with a high gain observer is designed to eliminate the unwanted deflection of the micro-cantilever beam system. The open-loop step response and the effects of situated places of PZT on the frequency responses of the system are discussed. Various frequency responses of the beam system, subject to different applied control voltages and feedback gains, are illustrated. The four resonances are well controlled, while the anti-resonance has little change. Computer simulations are provided to demonstrate the performance of the designed control scheme.

Keywords Adaptive vibration control · MEMS · Micro-cantilever · PZT

1 Introduction

Many micro-cantilever-beams-based MEMS (micro-electro-mechanical systems) instruments have been widely applied in modern technology, such as atomic force microscope (AFM), sensing sequence-specific DNA, detection of single electron spin, mass sensors, and chemical sensors [1–3].

The deflection of micro-cantilever beams is the key to scanning probe instruments, detection instruments, force measurements, magnetic spin detection, and thermal measurements [4]. The mechanical vibration and nonlinearities of the beam restrict the resolution of these instruments. Some researches have been conducted on the vibration and nonlinearities of MEMS in recent years. Franks [5] observed the effects of the uncertain vibration on the performance of atomic force microscope (AFM). Wang [6] considered many feedback control forms of vibration in a micro-machined cantilever beam with nonlinear electrostatic actuators. Cunningham et al. [7, 8] studied the application of vibration control to a fixed-free cantilever made of stainless steel with its length 16 mm, and the first two modes of vibration had been actively cancelled. Piezoelectric materials have coupled mechanical and electrical properties. Piezoelectric polymers and ceramics can be used to control the vibration of cantilever beams, such as most typical material polyvinylidene fluoride (PVDF) and PZT. However, for vibration control of a micro-cantilever beam under micron magnitude, thick PZT films and thin ZnO films should be considered [9, 10]. Weinberg [11] obtained a simple closed-form solution for the bending of piezoelectric multimorphs using Euler–Bernoulli beam theory, which neglects the effect of transverse shear on the deformation of the beam. Muralt [12] served piezoelectric layered beams as sensors and actuators in MEMS.

Therefore, it is very important to investigate the nonlinearities, vibration, and control of micro-cantilever beams in MEMS. The paper has the following structure. In Sect. 2, we present the dynamical model and the governing motion equation of a micro-cantilever beam with PZT and reduce the order of the system using Rayleigh–Ritz method in modal space. Section 3 discusses the design of a rational linearization feedback control with a high gain observer for this system. According to the analysis in Sects. 2 and 3, detailed computer simulation results are shown in Sect. 4 to visualize the control effects of the proposed approach. We end the paper in Sect. 5 with concluding remarks.

W. Zhang (✉) · G. Meng · H. Li
State Key Laboratory of Vibration, Shock and Noise,
Shanghai Jiao Tong University,
1954 Huashan Road, Shanghai 200030, People's Republic of China
E-mail: wenmingz@sjtu.edu.cn
Tel.: +86-21-54744990

Nomenclature

w	Micro-cantilever beam displacement
L	Micro-cantilever beam length

h_b Micro-cantilever beam thickness
h_p Piezoceramics thickness
A_b Micro-cantilever beam cross-sectional area
A_p Piezoceramics cross-sectional area
w_b Micro-cantilever beam width
w_p Piezoceramics width
C Micro-cantilever beam structural damping
d_{31} Piezoceramics constant
x_1 Inboard end of the actuator
x_2 Outboard end of the actuator
ε_p Strain induced by the actuator
ε_{lp} Longitudinal strain
M_p Bending moment induced by the actuator
E_b Young's modulus of micro-cantilever beam
ρ_b Density of micro-cantilever beam
E_p Young's modulus of Piezoceramics
ρ_p Density of Piezoceramics
δ Dirac delta function
ϕ_i Micro-cantilever beam mode shape function
q_i Micro-cantilever beam generalized coordinate
m_{ij} Inertia matrix
n_{ij} Beam viscous damping ratio matrix
k_{ij} Stiffness matrix
V Piezoelectric applied voltage
N Number of beam modes
ε Small positive design parameter
e_i Estimate error
b_i Feedback gain
d_i Observer gain
ζ Damping ratio
t Time

Subscripts:
b Micro-cantilever beam
p Piezoceramics actuator

2 Dynamical model and governing equations

The paper considers a micro-cantilever beam with a piezoceramics actuator sandwiched near the fixed end, as shown in Fig. 1. The governing equation of motion and boundary conditions for the transverse vibration of the uniform micro-cantilever beam, subject to a base excitation and a control bending moment applied by the actuator, is obtained using Hamilton's principle as:

$$\frac{\partial^2}{\partial x^2}\left[EI\frac{\partial^2 w(x,t)}{\partial x^2}\right]+C\frac{\partial w(x,t)}{\partial t}+\rho A\frac{\partial^2 w(x,t)}{\partial t^2} = \frac{\partial M_P(x,t)}{\partial x}-f(x,t)\,, \tag{1}$$

with boundary conditions

$$w(0,t)=\left.\frac{\partial w(x,t)}{\partial x}\right|_{x=0}=0;$$
$$EI\left.\frac{\partial^2 w(x,t)}{\partial x^2}\right|_{x=L}=EI\left.\frac{\partial^3 w(x,t)}{\partial x^3}\right|_{x=L}=0\,. \tag{2}$$

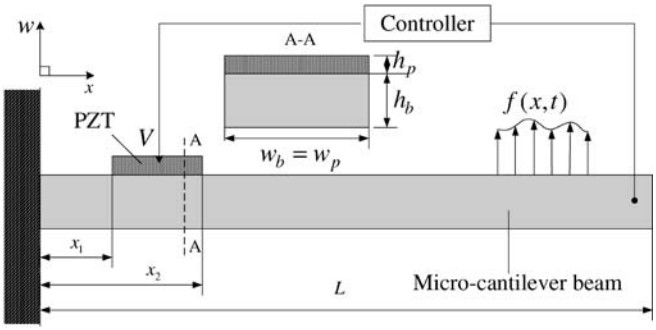

Fig. 1. Micro-cantilever beam model

Assuming that the actuator is bonded perfectly to the beam, the induced moment distribution, $M_p(x,t)$, between the actuator and beam surfaces can be calculated by Kirchoff's hypothesis. The strain induced by the actuator when a control voltage $V(x,t)$ is applied is given by [13, 14]:

$$\varepsilon_p(x,t)=\frac{d_{31}}{h_p}V(x,t)\,. \tag{3}$$

This induced strain ε_p creates a longitudinal strain ε_{lp} due to the force equilibrium. Solving the force equilibrium, we obtain the longitudinal strain:

$$\varepsilon_{lp}=\frac{E_pA_p}{E_bA_b+E_pA_p}\varepsilon_p\,. \tag{4}$$

The bending moment M_p, produced by the piezoceramics actuator, can be attained from Eqs. 3 and 4 under consideration of the force equilibrium in the axial direction:

$$M_p = E_bh_bw_b\varepsilon_{lp}\left(\frac{h_p}{2}-C_A\right) - E_ph_pw_p(\varepsilon_p-\varepsilon_{lp})\left(\frac{h_p}{2}+h_b-C_A\right)\,, \tag{5}$$

where C_A is the neutral axis of section $A-A$ given by:

$$C_A=\frac{E_bh_b^2w_b+E_ph_p^2w_p+E_ph_ph_bw_p}{2\left(E_bh_bw_b+E_ph_pw_p\right)}\,. \tag{6}$$

Substituting Eqs. 3, 4, and 6 into Eq. 5 gives:

$$M_p=C_0V(x,t)\,, \tag{7}$$

where

$$C_0=\frac{E_bE_ph_b^2w_bw_pd_{31}}{E_bh_bw_b+E_ph_pw_p}\,.$$

Then, the micro-cantilever beam equation of motion can be rewritten as:

$$\frac{\partial^2}{\partial x^2}\left[EI\frac{\partial^2 w(x,t)}{\partial x^2}\right]+C\frac{\partial w(x,t)}{\partial t}+\rho A\frac{\partial^2 w(x,t)}{\partial t^2} = C_0V(x,t)[\delta'(x-x_1)-\delta'(x-x_2)]-f(x,t)\,. \tag{8}$$

Note that $\delta'(x)$ is the derivative of the Dirac delta function with respect to x.

We suppose the piezoceramics have a uniform geometry and a spatially steady voltage is applied along its length. To obtain the solution of Eq. 8, $w(x,t)$ is expanded in a finite series using the Rayleigh–Ritz method:

$$w(x,t)=\sum_{i=1}^{N}\phi_i(x)q_i(t)\quad(i=1,2,\cdots,N)\,, \tag{9}$$

where $\phi_i(x)$ are mode shape functions and $q_i(t)$ are time-dependent, displacement generalized coordinates. Substituting Eq. 9 into Eq. 8 and integrating over the length, and divided by $\rho_b A_b$, the governing equations of the micro-cantilever beam are given:

$$m_{ij}\ddot{q}_j+2n_{ij}\dot{q}_j+k_{ij}q_j=Q_j+R_jV\quad(i,j=1,2,\cdots,N)\,, \tag{10}$$

where

$$\left.\begin{aligned}
m_{ij}&=\int_0^L\phi_i(x)\phi_j(x)\,\mathrm{d}x+\tfrac{\rho_pA_p}{\rho_bA_b}\int_{x_1}^{x_2}\phi_i(x)\phi_j(x)\,\mathrm{d}x\\
n_{ij}&=\tfrac{C}{2\rho_bA_b}\left(\int_0^L\phi_i(x)\phi_j(x)\,\mathrm{d}x+\int_{x_1}^{x_2}\phi_i(x)\phi_j(x)\,\mathrm{d}x\right)\\
k_{ij}&=\tfrac{E_bI_b}{\rho_bA_b}\int_0^L\tfrac{d^2\phi_i(x)}{\mathrm{d}x^2}\cdot\tfrac{d^2\phi_j(x)}{\mathrm{d}x^2}\,\mathrm{d}x+\tfrac{E_pI_p}{\rho_bA_b}\int_{x_1}^{x_2}\tfrac{d^2\phi_i(x)}{\mathrm{d}x^2}\cdot\tfrac{d^2\phi_j(x)}{\mathrm{d}x^2}\,\mathrm{d}x\\
Q_j&=-\tfrac{1}{\rho_bA_b}\int_0^L f(x,t)\,\mathrm{d}t\\
R_j&=\tfrac{1}{\rho_bA_b}C_0[\phi_j'(x_2)-\phi_j'(x_1)]
\end{aligned}\right\}. \tag{11}$$

The integrals in the first terms of m_{ij}, n_{ij}, and k_{ij} create only diagonal terms due to the orthogonality of $\phi_i(x)$ over the interval $[0,L]$, where L is the length of the beam. At the same time, the integrals in the second terms contribute to both diagonal and off diagonal terms because $\phi_i(x)$ are not orthogonal over the internal $[x_1,x_2]$. When the integrals in the second terms are neglected, as is usually the case, m_{ij}, n_{ij}, and k_{ij} are diagonal, and the equations of motion of the micro-cantilever beam are uncoupled.

3 Adaptive control

Introduce the state vector $x=[q^T,\dot{q}^T]^T\in R^{2N}$, then, the governing equations of motion become:

$$\dot{x}=Ax+Bu=\begin{bmatrix}0_{N\times N} & I_{N\times N}\\ -M^{-1}K & -M^{-1}D\end{bmatrix}x+\begin{bmatrix}0_{N\times 1}\\ M^{-1}F\end{bmatrix}u\,, \tag{12}$$

where M, K, and D are mass, stiffness and damping whose elements are shown in Eq. 11 and $D=\frac{2n_{ij}}{m_{ij}}$. F can be obtained from Eq. 10 as:

$$F=Q_j+R_jV\,. \tag{13}$$

To control the displacement of the micro-cantilever beam, we design the control system based on the modeling error compensation method by a high gain observer [15, 16].

For the control of vibration displacement, we induce an output variable:

$$y=Hx\,, \tag{14}$$

where $H=[\phi_1(L),\phi_2(L),\cdots,\phi_N(L)\ \ 0_{1\times N}]$. The feedback linearization of the input and output, from Eqs. 12 and 14, yields:

$$\ddot{y}=hx+gu\,, \tag{15}$$

where $h=HA^2$ and $g=HAB$, and the relative degree of y is two. From Eq. 15, we obtain a linearization feedback control:

$$u=g^{-1}(\ddot{y}-hx)\,. \tag{16}$$

Supposing the tracking error $\tilde{y}=y-\hat{y}$, and substituting it into Eqs. 15 and 16, gives:

$$\ddot{\tilde{y}}+b_1\dot{\tilde{y}}+b_2\tilde{y}=0\,, \tag{17}$$

where $b_1,b_2>0$, and the system Eq. 17 satisfies with stable conditions. Then, the tracking error agrees to $\tilde{y}=\lim_{t\to\infty}[y-\hat{y}]\to 0$. It is indicated that Eq. 17 can be determined by the system parameters. In MEMS, there exist many uncertainties from inherent factors to exterior excitations. Therefore, it is unlikely to get the exact expression for the tracking error.

In order to make a rational modification in Eq. 17, we induce compensation of the unknown terms in Eq. 15 and assume that:

$$g=g^*+\Delta g\,,\ h=h^*+\Delta h\,, \tag{18}$$

where g^* and h^* are known constants, which can be calculated using some parameters of the system, Δg is an unknown constant, and Δh is an unknown vector.

Substituting Eq. 18 into Eq. 15, we obtain:

$$\ddot{\tilde{y}}=-\ddot{\hat{y}}+g^*u+\tilde{h}^*y+S(x,u)\,, \tag{19}$$

where $\tilde{h}^*=h^*/H$ and $S(x,u)=\Delta hx+\Delta gu$.

Since the system Eq. 19 includes the unknown term $S(x,u)$, it is important to estimate its effect on the system and reconstruct state variables for the system. We regard the unknown term $S(x,u)$ as a state variable and induce state vector $z=[z_1\ z_2\ z_3]^T$, and $z_1=\tilde{y}$, $z_2=\dot{\tilde{y}}$, $z_3=S(x,u)$. Thus, Eq. 19 can be rewritten in state space as:

$$\dot{Z}=\begin{bmatrix}\dot{z}_1\\ \dot{z}_2\\ \dot{z}_3\end{bmatrix}=\begin{bmatrix}z_2\\ z_3-\ddot{\hat{y}}+\tilde{h}^*y+g^*u\\ \dot{S}(x,u)\end{bmatrix}\,. \tag{20}$$

To estimate the error term b_1,b_2, we construct a high gain observer, with the advantage that the estimation error converges to zero in a very small period. From the state Eq. 20, we determine an observer with the following form:

$$\dot{e}=\begin{bmatrix}\dot{e}_1\\ \dot{e}_2\\ \dot{e}_3\end{bmatrix}=\begin{bmatrix}\varepsilon d_2(z_1-e_1)+e_2\\ \varepsilon^2d_1(z_1-e_1)+z_3-\ddot{\hat{y}}+\tilde{h}^*y+g^*u\\ \varepsilon^3d_0(z_1-e_1)\end{bmatrix}\,, \tag{21}$$

where $d_0, d_1, d_2 > 0$, ε is a small positive design parameter, and e_i are the estimates of z_i $(i = 1, 2, 3)$, respectively. In addition, the parameters d_0, d_1, d_2 are chosen in terms of the polynomial:

$$\prod(s) = s^3 + d_2 s^2 + d_1 s + d_0 \,. \tag{22}$$

Therefore, according to Eq. 19 and using the estimate of the unknown function $S(x, u)$, we obtain a linearization feedback control for the micro-cantilever beam system with piezoelectric actuator:

$$u = (g^*)^{-1}(\ddot{\tilde{y}} - \tilde{h}^* y - b_2 \tilde{y} - b_1 e_2 - e_3) \,. \tag{23}$$

4 Simulation results

The geometry and material properties of the micro-cantilever beam and piezoelectric actuator are listed in Table 1. For convenience, we set the exterior load $f(x, t)$ to zero. In this computer simulation, we consider four modes of the vibration system.

Micro-cantilever beams have higher frequencies and Q values. To investigate the impacts of PZT on the beam system, the first ten modal frequencies of the beam with and without PZT are computed and the mode shapes are simulated using ANSYS 7.0, as listed in Table 2 and shown in Figs. 2 and 3. It could be seen that the relative errors of the first ten modal frequencies of the beam with and without PZT are very small and the mode shapes are approximate. Part mode shapes (mode 1, 4, 7, 10) of the beam with and without PZT are shown in Figs. 2 and 3, we find the differences between them are trivial.

Figure 4 shows the open-loop response for the step input of $V = 10v$ with initial conditions of $q = \dot{q} = 0$ and the structural damping D in Eq. 12 is set to zero. For $D = 0$, the zeros of the system are on the imaginary axis and the zeros dynamics are only marginally stable. At the same time, the open-loop response for the step input of $V = 10v$ and damping ratio $\zeta = 0.001$ is illustrated in Fig. 5. Since the effects of damping on micro-cantilever beam in MEMS cannot be ignored in micro-scale, we consider the damping in the following simulations to keep the system stable.

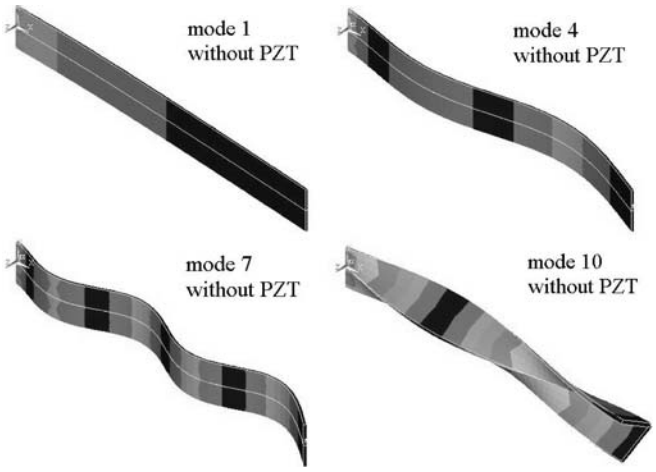

Fig. 2. Part mode shapes of the beam without PZT (mode 1, 4, 7, 10)

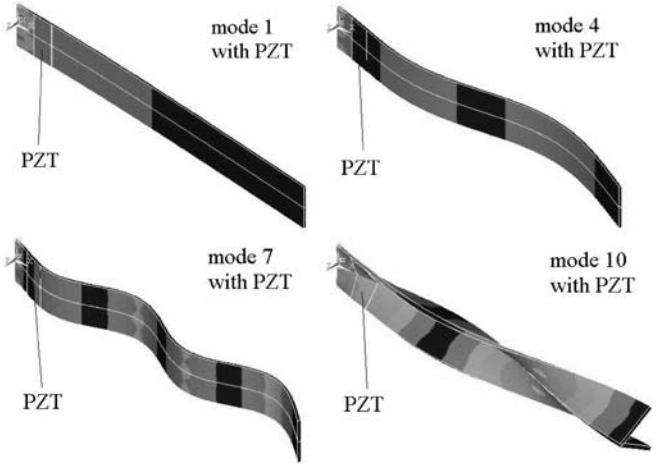

Fig. 3. Part mode shapes of the beam with PZT (mode 1, 4, 7, 10)

Figure 6 shows the frequency responses of the beam with PZT situated at different places for $V = 10v$. When the PZT are located at 30 μm, 100 μm, and 200 μm, the first two modes changes obviously and are larger, while mode 3 and mode 4 vary regularly and are smaller. The anti-resonances of the first two

Table 1. Geometric and material properties of micro-cantilever beam and piezoelectric actuator

	Material	Length (μm)	Width (μm)	Thickness (μm)	Density (kg/m^3)	Young's modulus (GPa)	Piezoelectric constant (m/V)
Cantilever beam	S_iO_2	500	30	3	2330	107	—
Actuator	PZT	30	30	0.5	7500	139	123×10^{-12}

Table 2. Mode frequencies of the micro-cantilever beam without and with PZT (kHz)

Number of mode	1	2	3	4	5	6	7	8	9	10
Beam without PZT	12.697	79.853	126.93	224.49	441.63	442.13	735.29	788.66	1106.3	1332.7
Beam with PZT	12.977	80.168	127.13	223.41	439.09	450.74	732.09	785.57	1106.3	1356.5
Relative error	2.21%	3.94%	0.16%	-0.48%	-0.58%	1.95%	-0.44%	-0.39%	0	1.79%

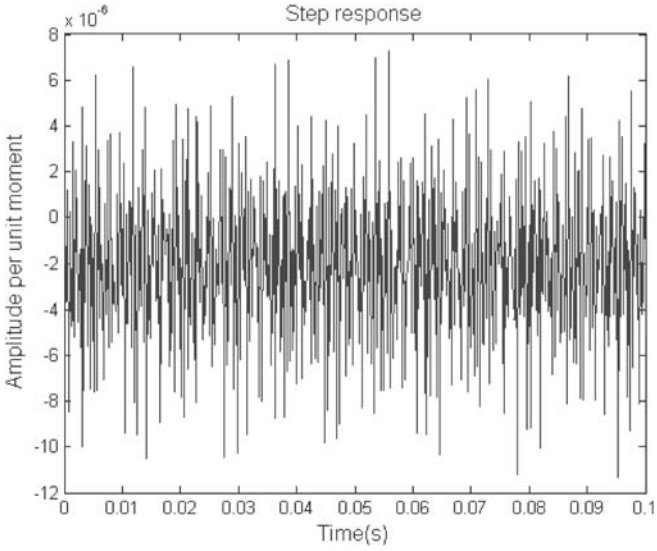

Fig. 4. Open-loop step response of beam with PZT for $V = 10v$

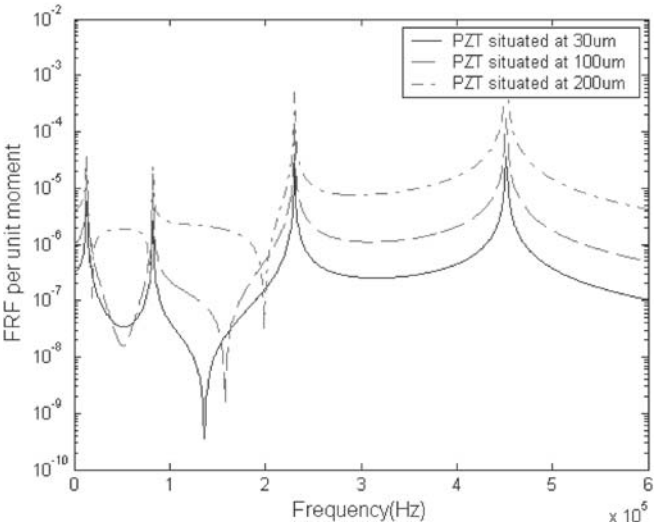

Fig. 6. Frequency response of the beam with PZT situated at different places for $V = 10v$

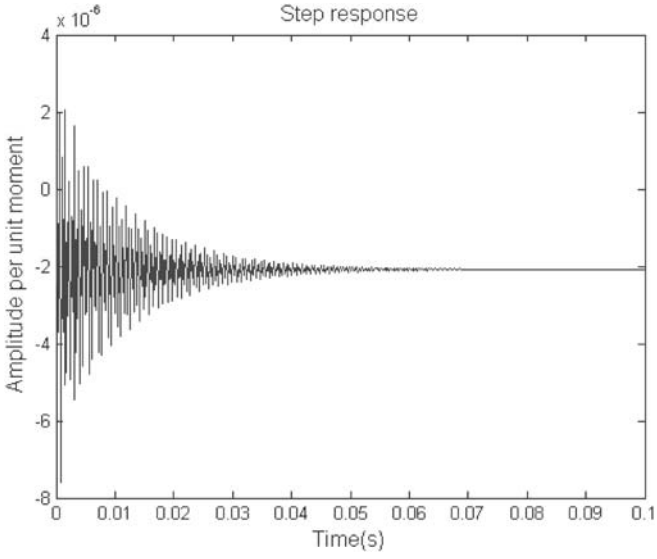

Fig. 5. Open-loop step response of beam with PZT for $\zeta = 0.001$ and $V = 10v$

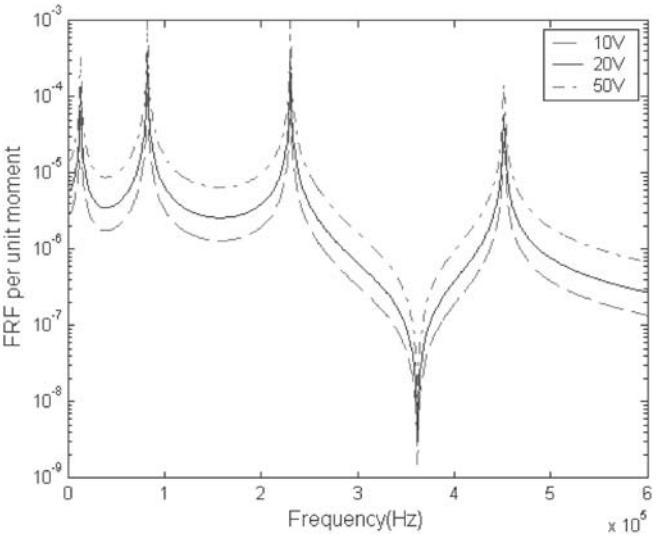

Fig. 7. Frequency response of the beam with PZT under different voltages

modes change sharply and appear as two anti-resonances when the PZT are situated at 100 μm and 200 μm, while there exists one anti-resonance that changes gently when the PZT are situated at 30 μm. It is seen that PZT placed near the clamped end of the beam gives better performance and correspondingly smaller resonances.

The frequency response of the beam with PZT under different control voltages is illustrated in Fig. 7. For various applied voltages, clear resonant behavior is still apparent around the nature frequencies. Along with the increase of the voltage, the resonant amplitude increases proportionally.

To get the simulation results of the micro-cantilever beam model Eq. 12 with the adaptive control law Eq. 23 using the high gain observer Eq. 20, we establish stability in the closed-loop system and select the feedback gains, b_1, *and* b_2, in Eq. 23 by placing the appropriate poles in the complex plane. With feedback gains, $b_1 = b_2 = 10$, we can ensure poles of Eq. 17 at the imaginary half plane. The initial conditions for the observer are chosen to be $z_1(0) = z_2(0) = z_3(0)$. The parameter ε has a significant effect on the performance of the system. For a smaller value of ε, we can estimate the uncertain factors quickly. Here, we select the value of ε as 0.000001 to confirm that the estimate error is less than 1%.

Figures 8 and 9 display the frequency responses of the beam with PZT after the application of the linearization feedback controller using a high gain observer for $V = 10v$ and $V = 50v$, respectively. Without control, clear sharp resonances can be observed. After output feedback control, the three highest modes are clearly well controlled, while the remainder are virtually un-

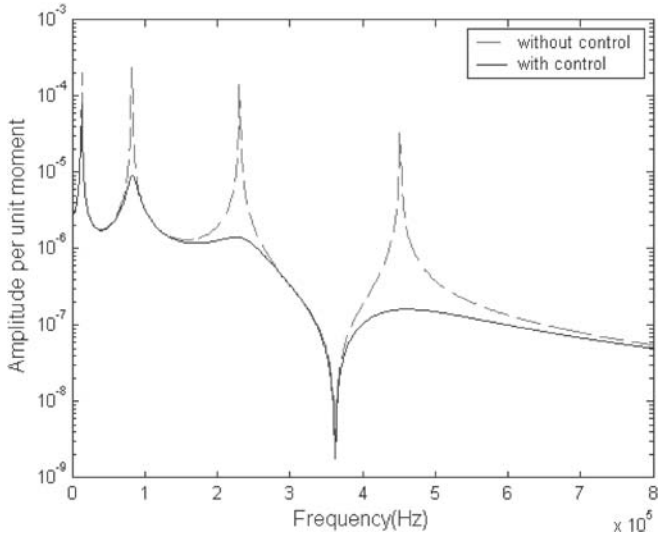

Fig. 8. Frequency response of the beam with PZT for $V = 10v$

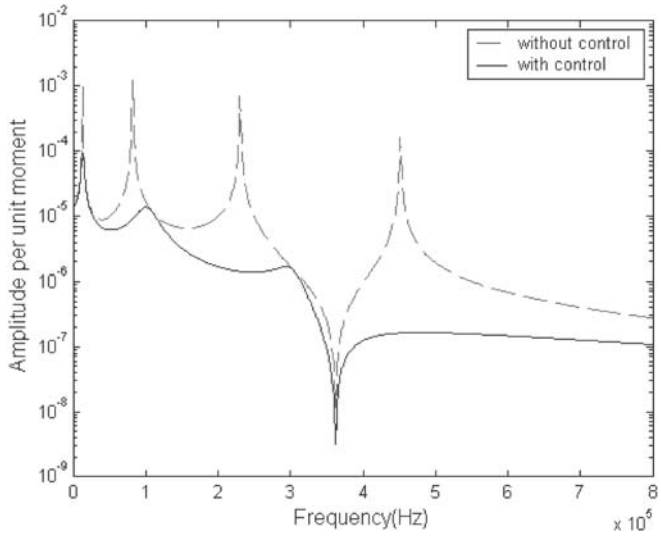

Fig. 9. Frequency response of the beam with PZT for $V = 50v$

affected, and the anti-resonant mode even has no change. Sharp resonances are associated with the uncontrolled modes, therefore, they still exist or have no change. Involving more modes in the control design can alleviate this problem, but only at the cost of increasing modal complexity.

Figures 10 and 11 illustrate the frequency response of the beam with PZT for $V = 50v$ after setting the feedback gains, $b_1 = b_2 = 2$ and $b_1 = b_2 = 50$, respectively. The modes are obviously well controlled except for the anti-resonance around the nature frequency bands, as shown in Fig. 10. It is seen that the anti-resonance between mode 3 and mode 4 become very sharp in Fig. 11. Therefore, the selection of feedback gains for the system should take the functions and stability of the system into consideration. The rational values of the feedback gain are about 10 for this micro-cantilever beam system.

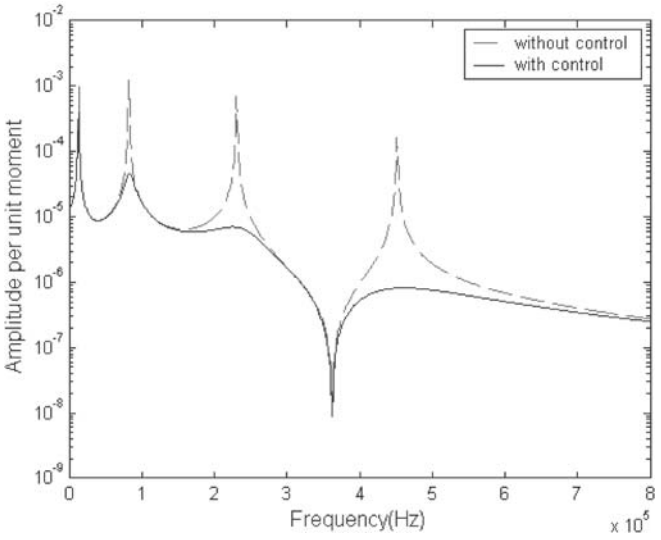

Fig. 10. Frequency response of the beam with PZT for $V = 50v$ and $b_1 = b_2 = 2$

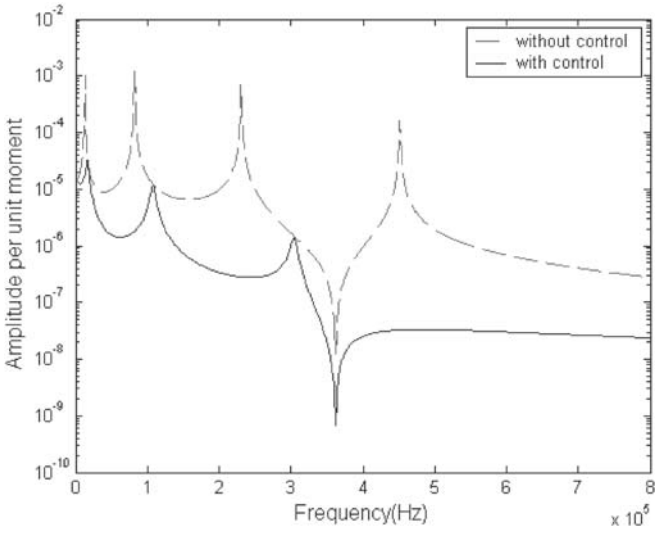

Fig. 11. Frequency response of the beam with PZT for $V = 50v$ and $b_1 = b_2 = 50$

5 Conclusions

The dynamical model of the micro-cantilever beams based MEMS with piezoelectric actuator (PZT) are presented. The order of the system is reduced using the Rayleigh–Ritz method in modal space. Comparing the beam model with and without PZT, it is apparent that the first ten modal frequencies and shapes are approximate and the relative error is very small. The reason for these similarities is that the beam system holds higher nature frequencies and Q values in the micro-scale. Based on a rigorous mathematical analysis and stability theory, a feedback controller with a high gain observer is designed so that one can effectively cancel the uncertain vibration of the beam system.

The open-loop step response and the effects of situated places of PZT on the frequency responses of the system are studied. Various frequency responses of the beam system are showed under different applied control voltages and feedback gains. The four resonances are well controlled, while the anti-resonance has no change. Simulation results demonstrate that the proposed design is able to achieve the control objective.

Acknowledgement The authors are grateful to Dr. K.X. Wei and X.J. Dong. This project was funded by the National Outstanding Youth Foundation of China (No.10325209).

References

1. Basso M, Giarre L, Dahleh M, Mezic I (1998) Numerical analysis of complex dynamics in atomic force microscopes. Proceedings of the IEEE International Conference on Control Applications, Trieste, Italy, 1–4 September 1998, pp 1026–1030
2. Fritz J, Baller MK, Lang HP, Rothuizen H, Vettiger P, Meyer E, Gntherodt HJ, Gerber C, Gimzewski JK (2001) Translating bio-molecular recognition into nanomechanics. Science 288:316–318
3. Sidles JA (1991) Noninductive detection of single proton-magnetic resonance. Appl Phys Lett 58(24):2854–2856
4. Ashhab M, Salapaka MV, Dahleh M, Mezic I (1999) Dynamical analysis and control of micro-cantilevers. Automatica 35:1663–1670
5. Franks A (1993) Progress towards traceable nanometric surface metrology. Nanotechnology 4:200–205
6. Wang PKC (1998) Feedback control of vibrations in a micromachined cantilever beam with electrostatic actuators. J Sound Vib 213(3):537–550
7. Jenkins DFL, Cunningham MJ, Clegg WW (1995) The use of composite piezoelectric thick films for actuation and control of miniature cantilevers. Microelectron Eng 29:71–74
8. Cunningham MJ, Jenkins DFL, Clegg WW, Bakush MM (1995) Active vibration control and actuation of a small cantilever for applications in scanning probe instruments. Sens Actuators A 50:147–150
9. Egusa S, Iwasawa NI (1993) Piezoelectric paint: preparation and application as built in vibration sensors of structural materials. J Mater Sci 28:1667–1672
10. Sayer M (1991) Piezoelectric thin film devices. Proceedings of the IEEE Ultrasonics Symposium, Honolulu, HI, 1991, pp 595–601
11. Weinberg MS (1999) Working equations for piezoelectric actuators and sensors. J Microelectromech Syst 8:529–533
12. Muralt P (2000) Ferroelectric thin films for micro-sensors and actuators: a review. J Micromech Microeng 10:136–146
13. Bailey T, Hubbard JE (1985) Distributed piezoelectric-polymer active vibration control of a cantilever beam. J Guid Control Dyn 8(5): 605–611
14. Baz A, Poh S (1988) Performance of an active control system with piezoelectric actuators. J Sound Vib 126(2):327–343
15. Aloliwi B, Khalil HK (1997) Adaptive output feedback regulation of a class of nonlinear system: convergence and robustness. IEEE Trans Autom Control 42(12):1714–1716
16. Khalil HK (1996) Adaptive output feedback control of nonlinear systems represented by input-output models. IEEE Trans Autom Control 41(2):177–188